Accepted Manuscript

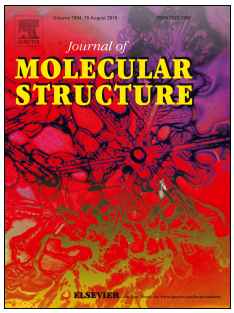

Phytotoxicity, structural and computational analysis of 2-Methyl-1,5-diarylpentadienones

Zia Ud Din, Edson Rodrigues-Filho, Viviane de Cassia Pereira, Sonia Cristina Juliano Gualtieri, Victor Marcelo Deflon, Pedro Ivo da Silva Maia, Aleksey E. Kuznetsov

PII: S0022-2860(17)30470-2

DOI: 10.1016/j.molstruc.2017.04.028

Reference: MOLSTR 23650

To appear in: *Journal of Molecular Structure*

Received Date: 4 November 2016

Revised Date: 10 April 2017

Accepted Date: 10 April 2017

Please cite this article as: Z.U. Din, E. Rodrigues-Filho, V. de Cassia Pereira, S.C.J. Gualtieri, V.M. Deflon, P.I. da Silva Maia, A.E. Kuznetsov, Phytotoxicity, structural and computational analysis of 2-Methyl-1,5-diarylpentadienones, *Journal of Molecular Structure* (2017), doi: 10.1016/j.molstruc.2017.04.028.

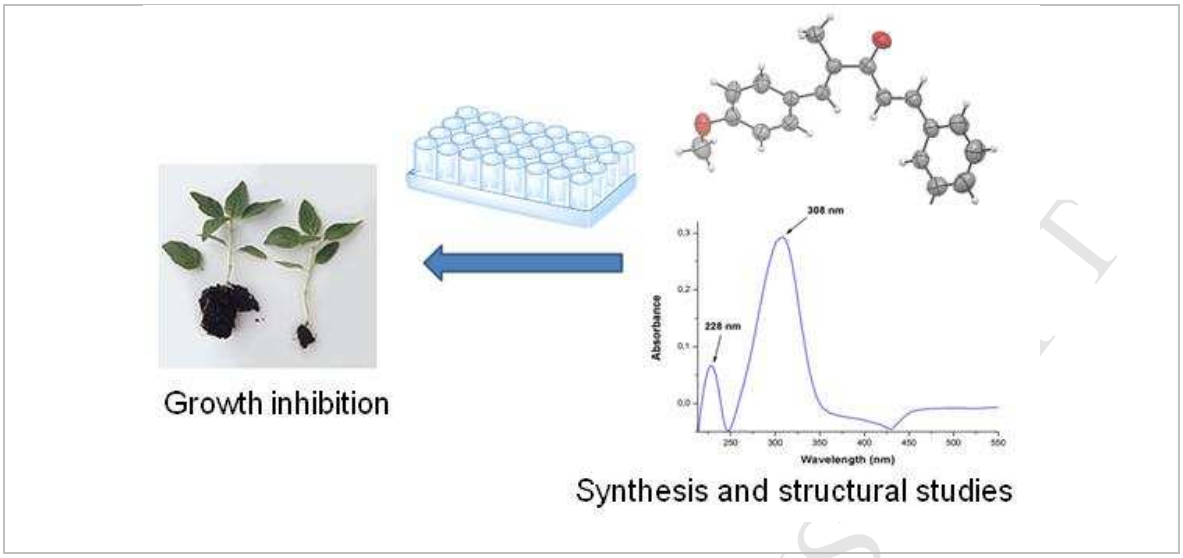

Phytotoxicity, Structural and Computational Analysis of 2-Methyl-1,5-diarylpentadienones

Zia Ud Din[a)], Edson Rodrigues-Filho[a)], Viviane de Cassia Pereira[b)], Sonia Cristina Juliano Gualtieri[b)], Victor Marcelo Deflon[c)], Pedro Ivo da Silva Maia[c)] and Aleksey E. Kuznetsov[*d)]

a) LaBioMMi, Departamento de Química, Universidade Federal de São Carlos, CP 676, 13565-905, São Carlos, SP, Brazil.

b) Laboratório de Ecofisiologia de Sementes, Universidade Federal de São Carlos, CP 676, 13565-905, São Carlos, SP, Brazil.

c) GQIEB, Instituto de Química de São Carlos, Universidade de São Paulo, 13566-590 São Carlos, SP, Brazil.

d) Instituto de Química, Universidade de São Paulo – SP, Av. Prof. Lineu Prestes, 748 – Butantã, 05508-000, São Paulo - SP – Brasil;

phone: +55(16)98109-6002; e-mail: aleksey73kuznets@gmail.com

Abstract: In our studies aimed to produce new chemicals used in weed control, 2-methyl-1,5-diarylpentadienones were synthesized by the reaction of *p*-methoxybenzaldehyde, *p*-nitrobenzaldehyde and *p*-*N*,*N*-dimethylbenzaldehyde, respectively, with 2-butanone, resulting in four model compounds. The phytotoxicity of these compounds against wheat coleoptiles and Sesame seedling was observed at µM concentrations, indicating good potential for their usage in weed management in the field. Spectroscopic and computational studies were performed in order to gain understanding on their mechanisms of action and to clarify some structural complexities due existence of conformers and substituent effects. These compounds probably act as hydroxyphenylpyruvate dioxygenase inhibitors. The tested compounds were characterized by spectroscopic and single crystal X-ray diffraction analyses. Solid crystalline state of the compound **A** (2-Methyl-1-(*p*-methophyphenyl)-5-(phenyl)-diarylpentadienone) is observed in the monoclinic space group $P2_{1/c}$ with unit cell dimensions a = 14.3366(4) Å, b = 11.3788(4) Å, c = 9.6319(3) Å, β = 96.596, V = 1560.88(9) Å^3 and Z = 4. Compound **C** (2-Methyl-1-(*p*-methophyphenyl)-5-(*p*-nitrophenyl)-diarylpentadienone) crystallizes in the monoclinic space group $P2_{1/c}$ with unit cell dimensions a = 17.8276(9) Å, b = 7.3627(4) Å, c = 12.9740(6) Å, β = 107.6230(10), V = 1623.04(14) Å^3 and Z = 4. LC-UV-MS analysis furnished important data helpful for their characterization. The spectroscopic data and computational (DFT) analysis revealed the fact that each of the compounds **A**-**D** occurs in solution as four conformers.

Keywords: Diarylpentadienone • Phytotoxic activity • XRD • Coleoptile

1. Introduction

The yield of agriculture products is dependent on control of the undesired plants, pests and weeds, which contribute negatively for crop yields. Approximately 7,000 weed species have been recognized until now; perhaps a few hundred of them are presenting troubles to the world's agriculturalists [1]. Although control of undesired plants using natural compounds have long being considered as a good and ecologically friendly approach, during the last 50 years researches have been focused almost exclusively on synthetic herbicides [2]. These compounds can be synthesized and optimized in laboratory for large scale production [3].

Different synthetic herbicides present at the market target the same biological process in weeds so their enormous use induces resistance in treated weeds. Due to this, the development of novel phytotoxic agents with different target processes has recently become a primary goal of the weed control research [4]. Potential phytotoxic agents are inspired by the vast variety of biologically active secondary metabolites of plants [5]. Phytological investigations have characterized some natural substances as good inhibitory agents [6], which disrupt mitochondrial function and cause apoptosis in *Arabidopsis* roots at concentrations as low as 35 μM [7].

Natural products chalcones and their precursors have exhibited good phytotoxic potential [8,9] causing programmed cell death in *Arabidopsis thaliana* roots [6,7]. The reduction of mitochondrial trans membrane potential was detected after chalcone treatment. Unsymmetrical 1,5-diarylpentadienones structurally resemble natural products chalcones possessing broad range of pharmacological properties. However, unsymmetrical 1,5-diarylpentadienones (Figure 1) have not been studied for their herbicide activity before. Their structure is composed of two aryl groups and a carbonyl group in conjugation with two C=C bonds. Diarylpentadienones and their congeners exhibited various biological activities such as antioxidant [10,11], cytotoxicity [12], anti-leishmanial activity [13], anti-tuberculous activity [14], antimalarial [15], antifungal [16], antifertility [17], antimitotic [18], antibacterial [19], and chemoprotective activity [20].

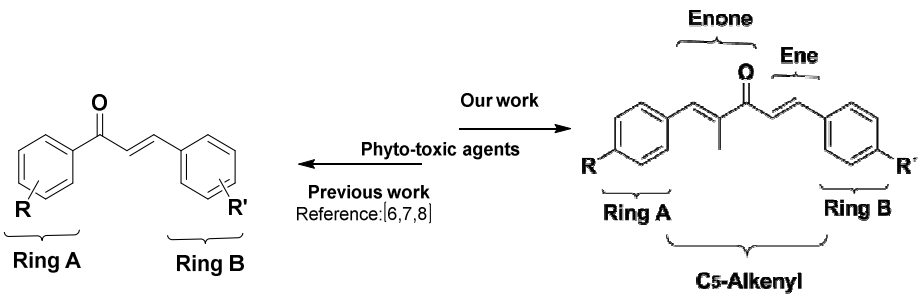

Figure 1. Comparison of the structure of 2-methyl-1,5-diarylpentadienones with chalcone.

The aim of this study is to discuss some interesting structural aspects of a series of diarylpentadienones recently produced and characterized by our research group, and also to evaluate their phytotoxic activity in order to gain understanding on their structural requirement to be potential herbicides. These compounds have different electron-donating and withdrawing groups affecting the dienone system, and analysis of the effects of these groups may help to understand the mechanism of inhibition. Docking studies were also carried out to predict the probability of binding of the compounds **A**-**D** with hydroxyphenylpyruvate dioxygenase (HPPD), a well-recognized important molecular target for inhibition of plant development. Moreover, theoretical calculations were performed to obtain detailed information about the possible conformations of the compounds **A**-**D**, which were revealed by LC-UV-MS analysis.

Compounds **A**-**D** were produced in two steps according to the scheme shown in Figure 2, by the reaction of anisaldehyde and *p*-*N*,*N*-dimethylbenzaldehyde with 2-butanone at first step to produce intermediate **1** and **2** [21]. After purification intermediate **1** was treated with benzaldehyde, *p*-*N*,*N*-dimethylbenzaldehyde, and *p*-nitrobenzaldehyde to yield compounds **A**, **B** and **C**, respectively. The intermediate **2** yields compound **D** by reacting with *p*-*N*,*N*-dimethylbenzaldehyde.

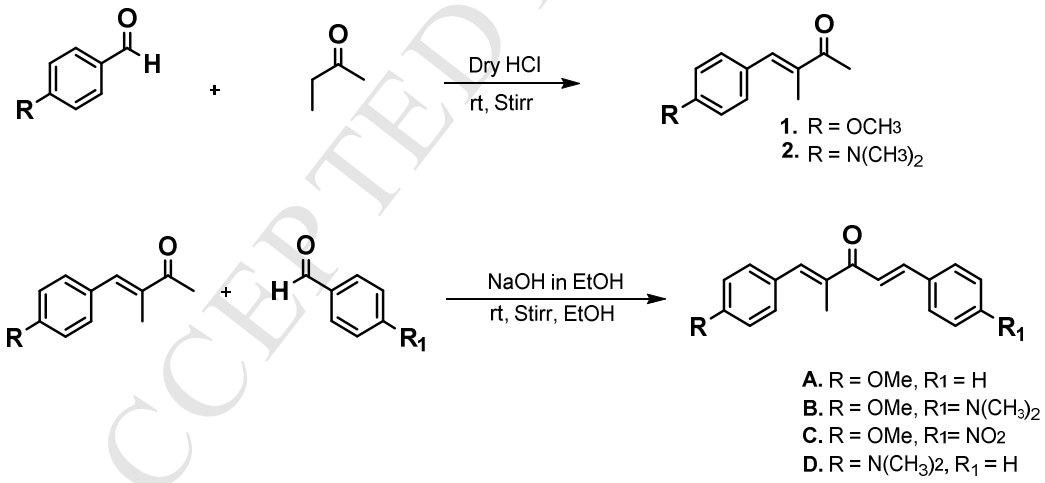

Figure 2. Synthetic scheme for 2-methyl-5-phenylpentadienones.

2. Material and Methods

2.1. Instrumentation

All chemicals were purchased from Organics, Sigma-Aldrich, Acros Chemicals and Fisher Scientific Ltda and used without further purification. The deuterated solvents of Apolo were used for the NMR

analysis. Thin layer chromatography was performed with precoated silica gel G-25-UV254 plates and detection was carried out at 254 nm under UV, and by vaniline in H_2SO_4 solution. Mass spectra (ESI-HRMS) were measured using a Thermo Scientific LTQ Orbitrap XL spectrometer operated at a resolution of 60,000 FWHM, in positive mode, *m/z* 90-800. HRMS/MS data were obtained by CID. ^{1}H NMR and ^{13}C NMR analyses were performed on a Brüker AVANCE 400 spectrometer operating at 400.15 MHz and 100.62 MHz, respectively. CDCl3 was used as a solvent and tetramethylsilane (TMS) as internal reference. Compounds **A-D** were dissolved in organic solvents at concentrations about 10 mg/mL each and placed into a 5-mm NMR tube. Chemical shifts (δ ppm) were measured with accuracy of 0.01 (^{1}H) and 0.1 ppm (^{13}C). The UV-vis spectra were recorded using a Perkin Elmer Lambda 25 spectrophotometer using 1 cm optical length quartz cuvettes at 25 °C and methanol as solvent. X-ray diffraction intensities were measured at room temperature (296 K) using Mo-K_α radiation (λ = 71.073 pm) on a Bruker APEX II Duo diffractometer.

2.2. Synthesis of the compounds A-D

Chalcone analogues can be formed by the direct reaction of aldehyde and ketone using basic or acid catalysis. Acid catalysts used for cross-aldol condensation reaction include sulfuric, hydrochloric [23] and Lewis acids. Compounds **1** and **2** were synthesized by treating anisaldehyde, and *p-N,N*-dimethylbenzaldehyde with 2-butanone in a 50 mL double-necked round bottom flask. Dry HCl gas was passed via the content of the flask until it was saturated and coloration appeared. The reaction mixture was stirred for 8 hrs. The crude product was diluted with toluene and washed with $NaHSO_3$ solution. The organic layer was separated, dried with anhydrous Na_2SO_4 and evaporated in vacuum. The residue was distilled under reduced pressure to give pure compound **1** and **2**, which were solidified by keeping in a refrigerator for 24 hrs. Intermediate compound **1** was further treated with benzaldehyde, *N,N*-dimethylbenzaldehyde and p-nitrobenzaldehyde, and yielded compounds **A-C**, while intermediate compound **2** was treated with benzaldehyde to yield compound **D**. All compounds were produced in a good yield and were characterized by different spectroscopic and spectrometric analyses (see Electronic Supporting Information).

A solution of **1** and **2** with aldehyde in ethanol (5 mL) was stirred for 5 minutes at room temperature and sodium hydroxide solution in ethanol (4 mL, 50 mmole) was added and the stirring was continued for 7 hrs. The solvent was evaporated in vacuum. Residue was dissolved in ethyl acetate, extracted with $NaHSO_3$ solution, dried with Na_2SO_4, and concentrated in vacuum yielding the crude product which was collected as precipitate and further purified by column chromatography and recrystallized from ethanol to give pure compounds **A-D**.

2.3. Growth of wheat coleoptile (Triticuma estivum) and Sesamum indicum

Wheat seeds (*Triticuma estivum*) were sown in Petri dishes (15 cm diameter) having one sheet of filter paper soaked with distilled water and grown in the dark at 22 °C for 3 days. Roots and caryopses were detached from the shoots. Shoots were placed in a Van der Weij guillotine, the apical 2 mm were cut off and discarded and the next 4 mm of the coleoptiles were recovered and used for the bioassay. This bioassay was performed to evaluate the initial growth of wheat coleoptile in the presence of compounds in concentrations 10^{-3} M; 3×10^{-4} M; 1×10^{-4} M, 3×10^{-5} M; and 10^{-5} M adopted from literature [24][25][26]. As a positive control, the herbicide Oxyfluorfen (240g/L) was used at the same concentrations. Seedling growth of sesame (*Sesamum indicum*) was carried by following methodology described by Grisi et al. [27]. The concentrations 10^{-3} M; 3×10^{-4} M; 1×10^{-4} M; 3×10^{-5} M and 10^{-5} M were used, and positive control herbicide Oxyfluorfen (240 g/L) was used at the same concentrations. All results were tested for normality and homoscedasticity with the Shapiro-Wilk and Levene tests, respectively. Normal and homoscedastic data were analysed with ANOVA followed by Tukey's test. The heteroscedastic data were analysed with the non-parametric Kruskal-Wallis test, in the software Past 2.14 [28].

2.4. X-ray characterization

Single crystals were grown by dissolving the compounds in 5 mL of hot ethanol and allowing them to grow at room temperature for 24 hrs. Yellow prisms suitable for single crystal diffraction were obtained and used for data collection. X-ray diffraction intensities were measured at room temperature (296 K) using Mo-K_α radiation (λ = 71.073 pm) on a Bruker APEX II Duo diffractometer. Standard procedures were applied for data reduction and absorption correction. The crystal structures were solved by direct methods using the SHELX97 program. All non-hydrogen atoms were refined with anisotropic displacement parameters with SHELXL97 [29]. The hydrogen atoms were calculated at idealized positions using the riding model option of SHELXL97.

2.5. Docking study

Molecular docking was carried out using Auto Dock Tool from Scripts Vina Research Institute [30]. Auto Dock is a suite of automated docking tools, designed to predict how small molecules such as substrates or drug candidates bind to a receptor of known 3D structure. Docking was used to predict

both ligand orientation and binding affinity. For docking analysis, first the ligands were optimized on the basis of energy by software Avogadro 1.1.1 [31]. Calculations were performed by removing water molecules first and adding polar hydrogen atoms using the option available in autodock tool. Gasteiger charges were also assigned for ligands and then the protein ligand were processed for obtaining file .pdbqt, which are input files for autodock 4.2. Enzyme *1TFZ* was optimized by considering only active site that occupied by inhibitors. The preferred orientation of ligands and receptor by the formation of stable complex was predicted in three dimensions. Binding energy interaction results were elucidated using Discovery Studio Visualiser 4.1 [32].

2.6. Computational methods

Computational studies of the compounds **A-D** were performed using the Gaussian09 package [33]. Geometries of all the species were optimized in the gas phase without any symmetry constraints. The resulting structures were assessed using vibrational frequency analysis to check whether the structures represent true minimum-energy geometries. If any imaginary frequency was detected, we performed further optimizations along the normal coordinates corresponding to the imaginary frequency(ies) (without symmetry constraints). For all the species under investigation, we studied four possible conformers, marked as **1-4** (see the manuscript text). All the calculations were done using the split-valence 6-311++G(d,p) basis set [34] containing the sets of polarization and diffuse functions on both heavier and hydrogen atoms, and the hybrid Becke three parameter hybrid functional with the non-local correlation provided by Perdew/Wang 91 B3PW91 [35,36]. This approach is subsequently referred to as B3PW91/6-311++G(d,p). For all the structures under investigation, we studied the singlet states and for some of them we checked triplet states as well (see discussion in the text and Electronic Supporting Information). To further refine the energies of the optimized conformers, we performed single-point calculations on the gas-phase optimized geometries using the B3PW91 functional and the Dunning's correlation consistent basis set cc-pVTZ [37]. In the paper, we discuss the results obtained in the gas phase without zero-point correction ZPE (ΔE_0). The charge analysis was performed using the Natural Bond Orbital (NBO) scheme with the 'pop=nbo' command as implemented in the Gaussian09 package [38,39]. Molecular structures and frontier orbitals were visualized using the OpenGL version of Molden 5.0 visualization software [40].

3. Results and Discussion

Although the 2D-draw of these diarylpentadienones seems to indicate simple molecular structures, there are some structural elements that render them some complexity due the possibility of existence of conformers, and this may impact their activities. Thus, during former works we have seen that the α-carbonylic and vinylic methyl group disturb the planarity of the cross-conjugated 1,5-diarylpentadienyl-3-one system [21], which open possibility for different contributions of substituents at the aromatic rings. Also, during some analysis of these compounds, the injection of dissolved pure and crystalline diarylpentadienones in the HPLC-UV-MS, with the column temperature set at 30 ^{o}C, at least four peaks are detected (data not shown here), being two major and two far minor peaks, with exactly same MS data, but differing in UV-absorption (e.g. **A**: major peaks with longer λmax at c.a. 315 and 335; minor peaks with shorter λmax at c.a. 280 and 290). The UV data of some of these compounds will be presented and discussed elsewhere. Here we presented the room temperature NMR data, where only the more stable conformers are seen; the MS/MS data at relatively low energy showing interesting fragmentation paths; their X-ray analysis; and their herbs inhibition activities along with a suggestion for their mechanism of action. Also a gas-phase conformational study is discussed.

3.1. NMR spectroscopic characterization

^{1}H NMR spectrum of compound **1** showed two characteristic signals of two methyl groups in the shielded region at δ_H 2.07 and 2.45, one methoxy singlet at δ_H 3.85, whereas one =CH was displayed at δ_H 7.39 as singlet; additionally, two aromatic signals having integration for four protons were detected at δ_H 6.93 and 7.41. ^{13}C NMR spectra of **1** showed signals for two methyl groups at δ_C 12.9 and 25.8, one OCH_3 at δ_C 55.3 and six peaks from δ_C 113–159 for eight carbons, with two of these peaks having double intensity for aromatic carbons. The characteristic peak at δ_C 200.3 is due to carbonyl carbon. The ^{1}H and ^{13}C NMR spectra of **1** and **2** are similar except the presence of the *N*,*N*-dimethyl substituent on benzene ring in **2** showed by signals at δ_H 3.02 and δ_C 40.15.

The reaction of the intermediate compound **1** with benzaldehyde, *N*,*N*-dimethylaminobenzaldehyde and *p*-nitrobenzaldehyde yields compounds **A**-**C**, respectively, while the reaction of *N*,*N*-dimethylaminobenzaldehyde with the compound **2** yields compound **D**. Also, extra signals in the aromatic region were noted in the ^{1}H spectra and the signal for methyl ketone group disappeared, showing that an aromatic ring was added and the methyl group was modified. The appearance of a pair of doublets at δ_H 7.53 and 7.69, with a coupling constant of c.a. 16 Hz, typical for two hydrogens in an E-double bound, clearly confirms that the aldol condensation with the second aldehyde occur. Further complete characterizations were performed by ^{1}H NMR, ^{13}C NMR, UV/Vis spectroscopy, mass spectrometry and X-ray analysis (for details, see Electronic Supporting Information).

Compounds **A**-**D** were produced in good yields after re-crystallization from ethanol: 51% for **A**, 93% for **B**, 69.3% for **C**, and 67% for **D**. The reaction progress was monitored by TLC. The reaction time depends on the nature of the aldehyde and substitution on it. Thus, for crossed aldol reaction, electron donors (*N,N*-dimethylamine) at the *p*-position in the benzene rings decrease the reaction time, while nitrobenzaldehyde reacted very fast.

3.2. Mass-spectral characterization

The mass-spectra profile of all four compounds revealed important and interesting fragmentation paths. The pseudomolecular ion peak ($[M+H]^+$) of the compound **A** ($C_{19}H_{18}O_2$, 278 Da) appeared at *m/z* 279.4 in its ESI(+)-MS/MS spectrum. Although these molecules demonstrate a high degree of unsaturation, which contributes for their stability, the MS/MS spectra, obtained when precursor ions were accelerated using relatively low energy (30 eV) for collisional induced dissociation (CID) against argon, contain interesting ion fragments which correlates well with their structures (see Electronic Supporting Information). Thus, the ions detected at *m/z* 121 and 91 were found related to the rings A and B of the compound **A**, which are formed from anisaldehyde and benzaldehyde, respectively. The peak at *m/z* 103 (100%) is due to production of styrene cation (path b). The cleavage that eliminates neutral phenyl ring results in the production of *m/z* 171.08 (path d). Well expected fragment ions were detected at *m/z* 77 (path i), 131 (path k) and 143 (path f). The acylium ions of *m/z* 131 and 143 were probably formed after ESI-protonation at C(2) or C(4) respectively, followed by cleavage of C(2) – C(3) or C(3) – C(4) bonds. The peaks that appeared at *m/z* 135 (path h) and 105 (path g) matches the formulas for methoxybenzoyl and benzoyl acyllium ions, although compound **A** does not have an oxygen atom directly attached to C(1) or C(5), respectively. These two apparently unexpected ions could be formed after ESI-protonation at C(2) or C(4), cyclization assisted by π-electrons from C=O forming an oxetane ring. Cleavages at this oxetane ring after H-rearrangement led to *m/z* 135 and 105 (Figure 3). The compounds **B**, **C** and **D** follow the same pattern. Their mass spectra are provided in the Electronic Supporting Information.

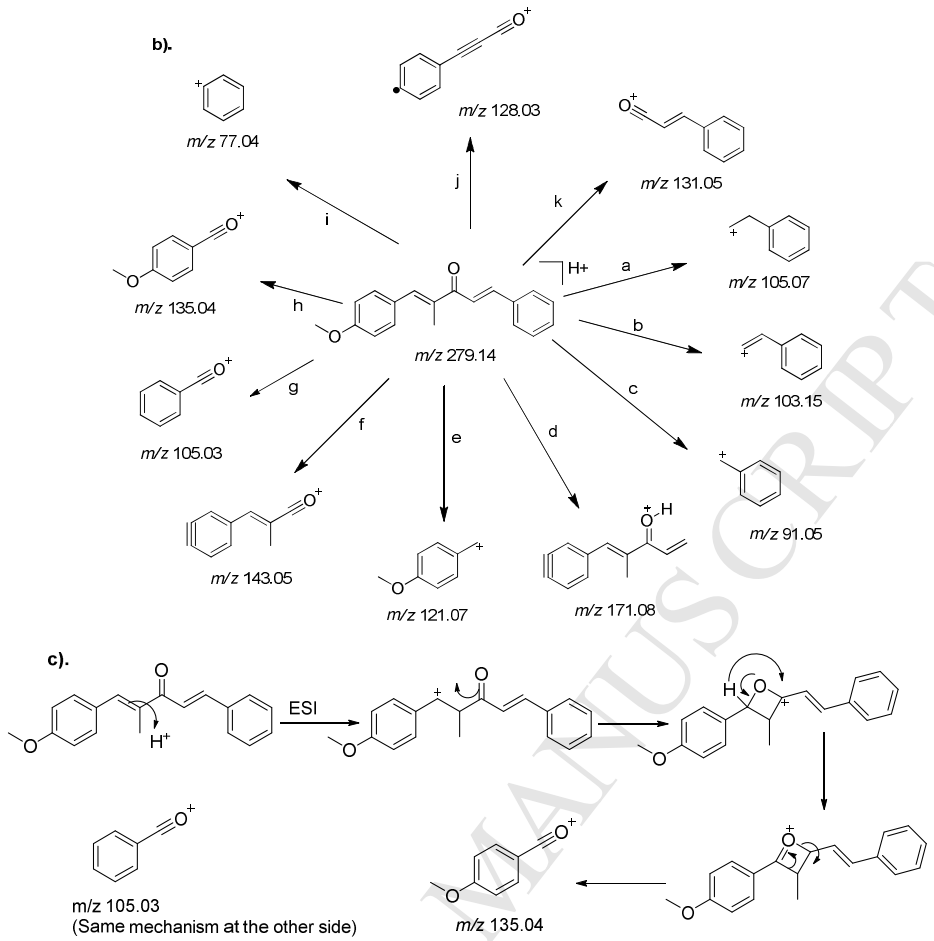

Figure 3. Fragmentation scheme followed for the compound **A** under collisional induced dissociation (CID) after ESI(+) ionization.

3.3. Crystallographic characterization

ORTEP drawings of the compounds **A** and **C** with numbering scheme are presented in Figure 4 and crystal packing diagram is shown in Figure S1. Selected bond distances and angles for these compounds are listed in Table S1 for understanding the effect of substitution upon the compound geometries The electron-donating and withdrawing groups significantly affect the bond distances and angles in compounds. The bond lengths along the carbon chain between the two aromatic rings are within the values for alternate single and double bonds. This alternation of single and double bonds makes the structure more flexible and less planar. The C(10)−O(1) bond is a typical double bond, which is in accord with the IR data. The bond distances N(1)−O(3) and N(1)−O(4) in the nitro group of **C** are exactly the same due to resonance inside this group. As expected, only weak interactions are observed in the crystal packing of these compounds. Detailed information about the structure determination is given in Table S2 (see Electronic Supporting Information).

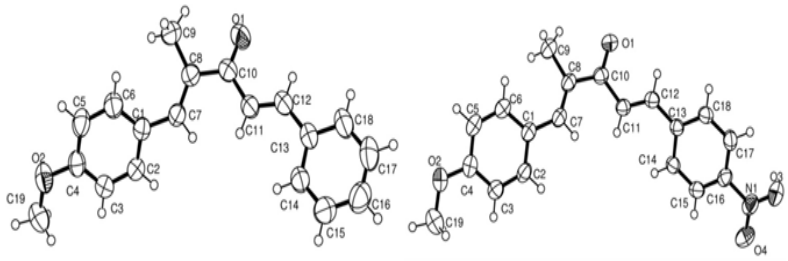

Figure 4. ORTEP structures and atomic numbering scheme for the compounds **A** (left) and **C** (right). Displacement ellipsoids for non-H atoms drawn at the 50% probability level.

3.4. Phytotoxic potential

The compounds studied induced inhibition of wheat coleoptiles growth in percentage compared to positive control Oxyfluorfen (Figure S2). All compounds had inhibitory effect at all concentrations tested on the growth of coleoptiles. However, the largest percentage of inhibition was caused by the compound **D** at the concentration of 10^{-3} M, while the compound **A** was the best inhibitor at lower concentration. Maybe **A**, being not very sensitive to pH variation compared to the compounds **B**-**D**, does not disturb molecular target by changing interacting site geometry when its concentration enhances.

Table S3 in Electronic Supporting Information shows comparison of the average of each treatment with the average obtained for the herbicide Oxyfluorfen treatment at different concentrations. It was noted that at all concentrations the effect of the herbicide is statistically similar to the effect caused by the compounds studied, except for the compound **B** at 3.10^{-5} M. Thus, we can say that these compounds have properties that resemble the herbicide. At the concentration of 10^{-4} M all the compounds **A**, **B**, **C**, and **D** were found to be more potent than the reference herbicide (Table S3).

Sesame seedlings grown in contact with the compounds **A** and **D** exhibited lower values of shoot and root length. The Figure S3 shows the average growth of the seedlings grown under the effect of these compounds. It was observed that only the concentration of 3.10^{-5} M did not inhibit the growth of shoots, since no significant difference was shown when compared with control treatment. The root seedling growth was compromised by the action of the compounds **A** and **D** at all concentrations tested, showing that these compounds have phytotoxic properties. Seedlings subjected to treatment with the herbicide Oxyfluorfen exhibited the lowest average growth of shoot and root at all concentrations tested.

3.5. Growth of cells of Sesamum indicum

The seedlings of metaxylem cells were exposed to the compounds **A** and **D** at the concentrations of 3.10^{-4} M and 10^{-5} M. The seedlings showed significant reduction in length by comparing with negative control treatment (Figure S4). The results of each treatment are also statistically compared in Table S4 (see Electronic Supporting Information). The cell lengths in the presence of the compounds **A** and **D** were measured to be 71.85 µm and 63.42 µm respectively for the first concentration and 95.47 µm and 79.40 µm for the second concentration, respectively. The average value of the control was 166.5 µm.

3.6. Herbicide compounds - HPPD enzyme docking studies

4-Hydroxyphenylpyruvate dioxygenase (HPPD) is a key enzyme present in plants that breaks down the amino acid tyrosine into components that plants utilize to create other molecules they need. Small molecular entities can act as HPPD inhibitors [22]. All the compounds **A-D** were analyzed for their binding capability to the enzyme HPPD *Pdb* (code *1TFZ*) and the results obtained are tabulated in Table S7. The active site calculation was carried out on the basis of the co-crystallized ligand in its crystal structure. Centroid of the active site was measured and then all compounds were evaluated for their *in silico* inhibition activity. The amino acids present in active sites and contributing actively are His-205, Pro-259, Asn-261, His-287, Met-314, Phe-360, Glu-373, Phe-398, Gly-399, Lys-400, Asn-402, and Phe-403. It is clear from the results obtained for the compounds **A**-**D** that they can have strong interactions with amino acids residues, like H-bonding, steric interactions, π-interactions and hydrophobic interactions. Compound **B** docked within the binding groove of HPPD with active residues. H bonding, π-interactions and hydrophobic interactions between the aromatic ring of **B** and that of amino acids residue in active pocket were observed (Figure 5). The results indicate that our curcuminoid analogues could be useful inhibitors of HPPD.

Compound **B** interacts with binding sites of amino acids with good fitting interactions. Hydrogen bonding was observed between the ligand with Asn-402 having distance 2.75 Å. The binding structure is given in Figure 5.

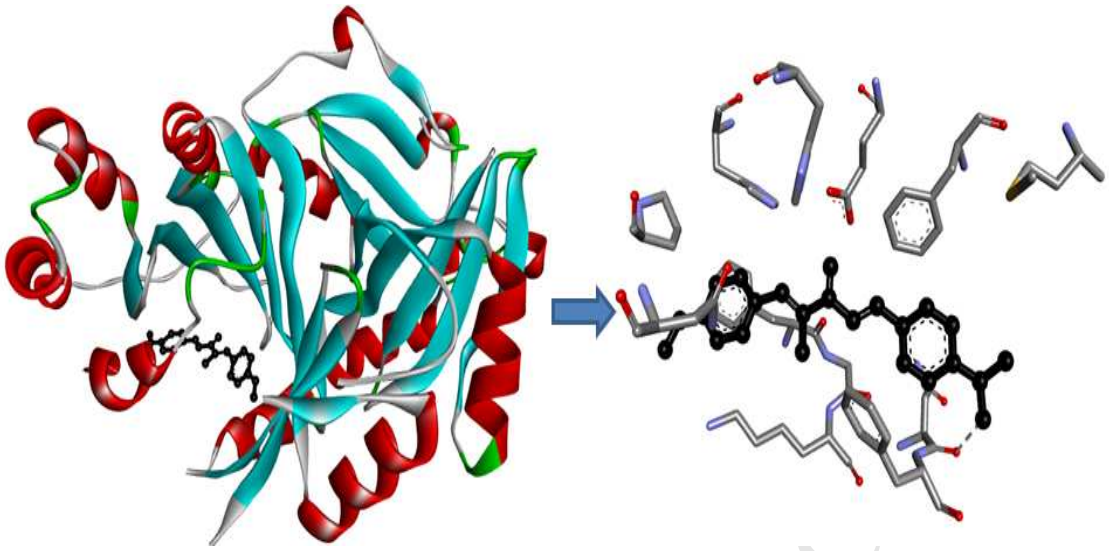

Figure 5. Docking diagram of the compound **B** with *1TFZ*.

3.7. Computational studies

The numbering system used in these discussions appears in Figure S5. Gas-phase optimized structures of the four conformers for each of the compounds studied are shown in Figure 6 as example, and in Figures S6-S8. The main energetic and structural features of the conformers of the compounds **A-D** are summarized below as follows:

(i) For all the four compounds, the singlet structures were found to be much lower in energy than the triplet structures. The triplet structure was calculated for the check purposes in the gas phase for the conformer **1** of the compound **A** (see Electronic Supporting Information, Table S5) and was found to be higher in energy by ca. 44 kcal/mol. Thus, in this study our focus was only on the singlet structures.

(ii) For the compound **A**, the conformer **1** (Figure 6) was found to be the most stable structure, whereas for the compounds **B-D** the conformer **3** (Figures S6-S8) was found to be the most stable species (see Electronic Supporting Information, Table S5). The conformer **1** has the both double bonds, C(7) – C(8) and C(11) – C(12) (see Figure 4 and Figure S5 for labeling), in trans-configuration and the atoms C(9) and O(1) in trans-position relative to each other. The conformer **3** also has the both double bonds in trans-configuration but the atoms C(9) and O(1) in cis-position relative to each other. Thus, it is possible to convert conformer **1** to conformer **3** simply by the rotation around the single bond C(8) – C(10). This is supported by the very small energy barriers between the conformers **1** and **3** for all the compounds **A-D**, ranging from 0.05 to 1.3 kcal/mol at the B3PW91/6-311++G(d,p) level (0.2-1.5 kcal/mol at the B3PW91/cc-pVTZ level of theory, see Table S5). Also, the almost negligible energy

difference between the conformers **1** and **3** of the compound **A** (0.05 kcal/mol) explains why the computed lowest-lying structure (**1**) differs from the experimentally found structure (**3**), see Figure 4.

(iii) For all the four compounds we found two or three very close lying in energy structures for the conformer **3** (see Figures S3-S6 and Table S5 in Electronic Supporting Information). The energy differences between these structures generally vary from 0.002 to 1.4 kcal/mol at the B3PW91/6-311++G(d,p) level and from 0.1 to 1.8 kcal/mol at the B3PW91/cc-pVTZ level of theory (see Table S5).

(iv) Interestingly, all the four calculated conformers for all the four compounds are quite close to each other in energy, the maximum energy differences (between the global minimum isomer, **1** or **3**, and isomer **4**) being 5.9-8.0 kcal/mol at the B3PW91/6-311++G(d,p) level and 6.7-8.9 kcal/mol at the B3PW91/cc-pVTZ level of theory (see Table S5).

(v) Geometry optimizations led to the noticeable structural distortions of the conformers **2-4** of all the four compounds (see Figures S6-S8), the deviations from planarity are especially noticeable for the conformers **2** and **4** of the compounds **A-D**. The conformer **2** has the double bond C(7) – C(8) in cis-configuration and the double bond C(11) – C(12) in trans-configuration and the atoms C(9) and O(1) in trans-position. The conformer **4** has the double bond C(7) – C(8) in trans-configuration and the double bond C(11) – C(12) in cis-configuration and the atoms C(9) and O(1) in trans-position.

(vi) The energy differences between the lowest-lying conformer **3** (**1** for the compound **A**) and the conformers **2** and **4** are quite noticeable, ranging from ca. 4 to 8 kcal/mol at the B3PW91/6-311++G(d,p) level (ca. 4-9 kcal/mol at the B3PW91/cc-pVTZ level), see Figures S6-S8 and Table S5 in Electronic Supporting Information. This is explained by the necessity to change the C=C bond(s) conformation to convert from the conformer **3** to **2**/**4**, thus the interchanging energy barriers are quite high in this case, compared to the interchange between **1** and **3**, see above.

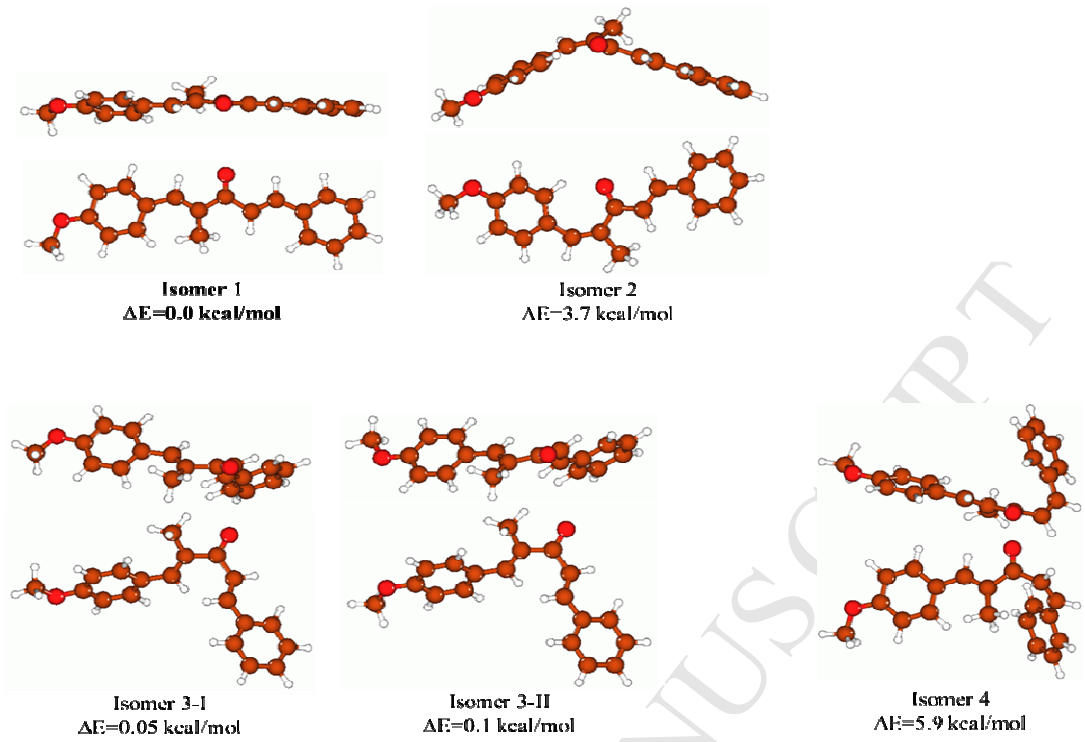

Figure 6. B3PW91/6-311++G(d,p) optimized gas phase structures of the isomers of compound **A**: side views (bottom rows) and top views.

Analysis of the electron density distribution in the lowest-energy isomers of the compounds **A**-**D**, as illustrated by the plots of the HOMOs (Figure 7), shows the following.

(i) The HOMOs of the compounds **A**, **C**, and **D** have dominating contributions from the double bond C(7) – C(8) and the benzene ring attached to it (including noticeable contributions from the electron-donating group CH_3O in the compounds **A** and **C** and electron-withdrawing group NO_2 in the compound **D**), along with some contributions from the O(1) and CH_3-group. The HOMO of the compound **B** has dominating contributions from the double bond C(11) – C(12) and the benzene ring attached to it, along with noticeable contributions from the electron-donating $N(CH_3)_2$ group and small contributions from the O(1) and the double bond C(7) – C(8).

(ii) Thus, the both double bonds in all the four compounds **A**-**D** bear quite significant amounts of the electron density, which is also supported by the results of the NBO analysis showing quite noticeable negative charges on the atoms C(7)-C(8) and C(11)-C(12) of the double bonds (see Table S6, Electronic Supporting Information). Also, large negative charges are accumulated on the carbonyl oxygen O(1) and the methyl group (C(9)). Therefore, the parts of the compounds **A**-**D** containing the double bonds should have significant reactivity towards various electrophiles, for example, towards positively charged amino acids residues or protons. The same should be true for the O- and N-

containing functional groups of these compounds. In total, the whole molecules of the compounds **A**-**D** should have strong interactions with amino acids residues, like H-bonding, steric interactions, π-interactions, and hydrophobic interactions, as described above in the section devoted to the docking studies.

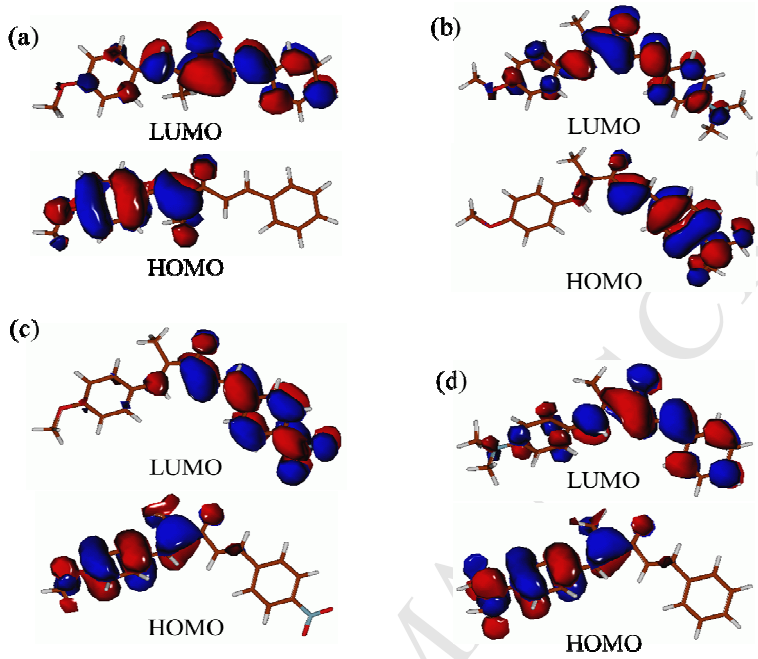

Figure 7. HOMOs and LUMOs of the lowest-energy conformers of the compounds **A** (a), **B** (b), **C** (c), and **D** (d).

4. Conclusions

The investigated compounds **A**, **B**, **C** and **D** were shown to exhibit impressive phytotoxic activity. These compounds are easy to synthesize and can be produced in desired amounts. Synthetic chalconoids can replace the natural herbicides due to difficult and time-consuming purification methods used to obtain those. The compounds **A**-**D** also show binding affinity to enzyme *1TFZ*, which may be the probable target for them. The DFT calculations provided valuable information on the structural and electronic features of **A**-**D**. Based on the computational results, we were able to determine the most stable conformers for each of the four compounds, make analysis of the electronic structures of the compounds studied, and thus provide explanations of their reactivity features. It seems that, at physiological conditions, the conformation mobility of these substances does not affect significantly their bioactivity.

Electronic Supporting Information

Electronic Supporting Information is free of charge. It contains the following data: NMR spectra of the compounds **1**, **2** and **A-D**; UV-vis spectra of the compounds **1**, **2** and **A-D**; mass spectra of the compounds **1, 2** and **A-D**; crystallographic information of the compounds **A - C**; phytotoxic properties of the compounds **A-D**; synthetic details of the compounds **1, 2** and **A-D**; details of computational studies of the compounds **A-D**; docking details of the compounds **A-D**.

Acknowledgements

The authors are grateful to Fundação de Amparo à Pesquisa do Estado de São Paulo (FAPESP), Conselho Nacional de Desenvolvimento Científico e Tecnológico (CNPq), and Coordenação de Aperfeiçoamento de Pessoal de Ensino Superior (CAPES) for financial su

pport and Third World Academy of Science (TWAS) for Ph.D. fellowship of ZUD. The computational resources of the Centro Nacional de Processamento de Alto Desempenho do CENAPAD-UFC in Fortaleza are highly apprecaited.

References

[1] S.O. Duke, 'Weed Physiology: Herbicide physiology, 1st ed., CRC Press, Mar 27 (1985) - Science - 272 pages. ISBN: 9780849363146.

[2] M.J. Kropff, H. Walter, EWRS and the challenges for weed research at the start of a new millennium, Weed Research 40 (1) (2000) 7-10. doi:10.1046/j.1365-3180.2000.00166.x.

[3] L.C.A. Barbosa, A.J. Demuner, C.R.A. Maltha, R.R. Teixeira, K.A.P. Souza, K.U. Bicalho, Phytogrowth Activity of 3-(3-Chlorobenzyl)-5-arylidenefuran-2(5H)-ones, Z. Naturforsch. 64 (b) (2009) 245-251. doi:10.1515/znb-2009-0216.

[4] F.E. Dayan, J.G. Romagni, S.O. Duke, Investigating the mode of action of natural phytotoxins, J. Chem. Ecology 26 (9) (2000) 2079-2094. doi:10.1023/A:1005512331061.

[5] S.O. Duke, A. Rimando, B. Scheffler, F.E. Dayan, in 'Allelopathy: from molecules to ecosystems', Ed. M.J. Reigosa, N. Pedrol, Science Publishers Inc., Einfield (2002) 139-152. ISBN: 1-57808-254-4

[6] H.R. Bitencourt, L.S. Santos, A.P.S. Souza Filho, Allelopathic activity of synthetic chalcone, its precursors and of related cetones and aldehydes, Planta Daninha 25 (4) (2007) 747-753. doi: 10.1590/S0100-83582007000400011.

[7] C. Díaz-Tielas, E. Graña, T. Sotelo, M.J. Reigosa, A.M. Sánchez-Moreiras, The natural compound trans-chalcone induces programmed cell death in *Arabidopsis thaliana* roots, Plant, Cell & Environment (35) (8) (2012) 1500-1517. doi:10.1111/j.1365-3040.2012.02506.x.

[8] C. Díaz-Tielas, T. Sotelo, E. Graña, M.J. Reigosa, A.M. Sánchez-Moreiras, Phytotoxic potential of trans-chalcone on crop plants and model species, J. Plant Growth Regulation (33) (2) (2013) 181-194. doi:10.1007/s00344-013-9360-6.

[9] A. Jitareanu, S. Padureanu, G. Tataringa, C. Tuchilus, U. Stanescu, Evaluation of phytotoxic and mutagenic effects of some cinnamic acid derivatives using the Triticum test, Turkish Journal of Biology (37) (4) (2013) 748-756. doi:10.3906/biy-1304-39.

[10] S. Handayani, I.S. Arty, Synthesis of hydroxyl radical scavengers from benzalacetone and its derivatives, J. Phys. Sci. (19) (2) (2008) 61-68.

[11] W.M. Weber, L.A. Hunsaker, S.F. Abcouwer, L.M. Deck, D.L. VanderJagt, Anti-oxidant activities of curcumin and related enones, Bioorg. Med. Chem. (13) (11) (2005) 3811-3820. doi: 10.1016/j.bmc.2005.03.035.

[12] J.R. Dimmock, M.P. Padmanilayam, G.A. Zello, K.H. Nienaber, T.M. Allen, C.L. Santos, E. De Clercq, J. Balzarini, E.K. Manavathu, J.P. Stables, Cytotoxic analogues of 2,6-bis(arylidene)cyclohexanones, Eur. J. Med. Chem. (38) (2) (2003) 169-177. doi:10.1016/S0223-5234(02)01444-7.

[13] S.F.P. Braga, E.V.P. Alves, R.S. Ferreira, J.R.B. Fradico, P.S. Lage, M.C. Duarte, T.G. Ribeiro, P.A. Júnior, A.J. Romanha, M.L. Tonini, M. Steindel, E.F. Coelho, R.B. de Oliveira, Synthesis and evaluation of the antiparasitic activity of bis-(arylmethylidene) cycloalkanones, Eur. J. Med. Chem. (71) (1) (2014) 282-289. doi:10.1016/j.ejmech.2013.11.011.

[14] N. Singh, J. Pandey, A. Yadav, V. Chaturvedi, S. Bhatnagar, A.N. Gaikwad, S.K. Sinha, A. Kumar, P.K. Shukla, R.P. Tripathi, A facile synthesis of alpha,alpha'-(EE)-bis(benzylidene)-cycloalkanones and their antitubercular evaluations, Eur. J. Med. Chem., 2009, 44, 1705–1709. doi:10.1016/j.ejmech.2008.09.026.

[15] S. Manohar, S.I. Khan, S.K. Kandi, K. Raj, G. Sun, X. Yang, A.D.C. Molina, N.N.B. Wang, D.S. Rawat, Synthesis, antimalarial activity and cytotoxic potential of new monocarbonyl analogues of curcumin, Bioorg. Med. Chem. Lett. (23) (1) (2013) 112-116. doi:10.1016/j.bmcl.2012.11.004.

[16] K.L. Lahtchev, D.I. Batovska, S.P. Parushev, V.M. Ubiyvovk, A.A. Sibirny, Antifungal activity of chalcones: a mechanistic study using various yeast strains, Eur. J. Med. Chem. (43) (1) (2008) 2220-2228. doi:10.1016/j.ejmech.2007.12.027.

[17] I.H. Hall, G.L. Carlson, G.S. Abernethy, C. Piantadosi, Cycloalkanones. 4. Antifertility activity, J. Med. Chem. (17) (12) (1974) 1253-1257. doi: 10.1021/jm00258a004.

[18] S. Ducki, R. Forrest, J.A. Hadfield, A. Kendall, N.J. Lawrence, A.T. McGown, D. Rennison, Potent antimitotic and cell growth inhibitory properties of substituted chalcones, Bioorg. Med. Chem. Lett. (8) (9) (1998) 1051-1056. doi:10.1016/S0960-894X(98)00162-0.

[19] D. Batovska, S. Parushev, B. Stamboliyska, I. Tsvetkova, Examination of growth inhibitory properties of synthetic chalcones for which antibacterial activity was predicted, Eur. J. Med. Chem. (44) (5) (2009) 2211-2218. doi:10.1016/j.ejmech.2008.05.010.

[20] H. Forejtníková, K. Lunerová, R. Kubínová, D. Jankovská, R. Marek, R. Kares, V. Suchý, J. Vondrácek, M. Machala, Chemoprotective and toxic potentials of synthetic and natural chalcones and dihydrochalcones in vitro, Toxicology (208) (1) (2005) 81-93. doi:10.1016/j.tox.2004.11.011.

[21] U.D. Zia, T.P. Fill, F.F. de Assis, D.B. Lazarin, V. Kaplum, F. Garcia, C.V. Nakamura, K.T. de Oliveira, E. Rodrigues-Filho, Unsymmetrical 1,5-diaryl-3-oxo-1,4-pentadienyls and their evaluation as antiparasitic agents, Bioorg. Med. Chem. (22) (3) (2014) 1121-1127. doi:10.1016/j.bmc.2013.12.020.

[22] G.R. Moran, 4-Hydroxyphenylpyruvate dioxygenase, Arch. Biochem. Biophys. (433) (1) (2005) 117-128. doi: 10.1016/j.abb.2004.08.015.

[23] S. Sardjiman, M. Reksohadiprodjol, L. Hakiml, H. van der Goo, H. Timmermanz, l,5-Diphenyl-1,4-pentadiene-3-ones and cyclic analogues as antioxidative agents. Synthesis and structure-activity relationship, Eur. J. Med. Chem. (32) (7-8) (1997) 625-630. doi: 10.1016/S0223-5234(97)83288-6.

[24] C.R. Barlow, H.W.B. Hancock, H.J. Lacey, The east malling coleoptile straight growth test method, J. Exp. Bot. (15) (43) (1964) 166-176. doi: www.jstor.org/stable/23687881.

[25] F.A. Macías, R. Lacret, R.M. Varela, C. Nogueiras, J.M. Molinillo, Isolation and phytotoxicity of terpenes from *Tectona grandis*, J. Chem. Ecol. (36) (4) (2010) 396-404. doi: 10.1007/s10886-010-9769-3.

[26] J.P. Nitsch, C. Nitsch, Studies on the growth of coleoptile and first internode sections. A new, sensitive, straight-growth test for auxins, Plant Physiol. (31) (2) (1956) 94-111. PMCID: PMC540740.

[27] P.U. Grisi, S.C.J. Gualtieri, S. Anese, V.C. Pereira, M.R. Forim, Effect of *Serjania lethalis* ethanolic extract on weed control, Planta Daninha (31) (2) (2013) 239-248. doi: 10.1590/S0100-83582013000200001.

[28] Ø. Hammer, D.A.T. Harper, P.D. Ryan, Paleontological statistics software package for education and data analysis, Palaeontologia Electronica (4) (2001) 1-9. http://palaeo-electronica.org/2001_1/past/issue1_01.htm.

[29] G.M. Sheldrick, SHELXL97, Program for the Refinement of Crystal Structures, University of Göttingen, Germany, 1997.

[30] O. Trott, A.J. Olson, AutoDock Vina: Improving the speed and accuracy of docking with a new scoring function, ffficient optimization, and multithreading, J. Comput. Chem. (31) (2) (2010) 455-461. doi:10.1002/jcc.

[31] M.D. Hanwell, D.E. Curtis, D.C. Lonie, T. Vandermeerschd, E. Zurek, G.R. Hutchison, Avogadro: An advanced semantic chemical editor, visualization, and analysis platform, J. Cheminformatics (4) (17) (2012) 1-17. doi: 10.1186/1758-2946-4-17.

[32] Dassault Systèmes BIOVIA, Discovery Studio Modeling Environment, Release 4.1, 2015.

[33] M.J. Frisch, G.W. Trucks, H.B. Schlegel, G.E. Scuseria, M.A. Robb, J.R. Cheeseman, G. Scalmani, V. Barone, B. Mennucci, G.A. Petersson, H. Nakatsuji, M. Caricato, X. Li, H.P. Hratchian, A.F. Izmaylov, J. Bloino, G. Zheng, J.L. Sonnenberg, M. Hada, M. Ehara, K. Toyota, R. Fukuda, J. Hasegawa, M. Ishida, T. Nakajima, Y. Honda, O. Kitao, H. Nakai, T. Vreven, J.A. Montgomery, Jr., J.E. Peralta, F. Ogliaro, M. Bearpark, J.J. Heyd, E. Brothers, K.N. Kudin, V.N. Staroverov, R. Kobayashi, J. Normand, K. Raghavachari, A. Rendell, J.C. Burant, S.S. Iyengar, J. Tomasi, M. Cossi, N. Rega, J.M. Millam, M. Klene, J.E. Knox, J.B. Cross, V. Bakken, C. Adamo, J. Jaramillo, R. Gomperts, R.E. Stratmann, O. Yazyev, A.J. Austin, R. Cammi, C. Pomelli, J.W. Ochterski, R.L. Martin, K. Morokuma, V.G. Zakrzewski, G.A. Voth, P. Salvador, J.J. Dannenberg, S. Dapprich, A.D. Daniels, Ö. Farkas, J.B. Foresman, J.V. Ortiz, J. Cioslowski, and D.J. Fox, Gaussian 09, Revision A.02, Gaussian, Inc., Wallingford CT, 2009.

[34] J.S. Binkley, J.A. Pople, W.J. Hehre, Self-consistent molecular orbital methods. 21. Small split-valence basis sets for first-row elements, J. Am. Chem. Soc. (102) (3) (1980) 339-347. doi: 10.1021/ja00523a008.

[35] A.D. Becke, Density□functional thermochemistry. III. The role of exact exchange, J. Chem. Phys. (98) (7) (1993) 5648-5652. doi: 10.1063/1.464913

[36] R.G. Parr, W. Yang, 'Density-Functional Theory of Atoms and Molecules', Oxford University Press, 1989.

[37] T.H. Dunning Jr., Gaussian basis sets for use in correlated molecular calculations. I. The atoms boron through neon and hydrogen, J. Chem. Phys. (9) (2) (1989) 1007-1023. doi: 10.1063/1.456153.

[37] R. Bauernschmitt, R. Ahlrichs, Treatment of electronic excitations within the adiabatic approximation of time dependent density functional theory, Chem. Phys. Lett. (256) (4-5) (1996) 454-464. doi: 10.1016/0009-2614(96)00440-X.

[38] A.E. Reed, L.A. Curtiss, F. Weinhold, Intermolecular interactions from a natural bond orbital, donor-acceptor viewpoint, Chem. Rev. (88) (6) (1988) 899-926. doi: 10.1021/cr00088a005.

[39] A.E. Reed, R.B. Weinstock, F. Weinhold, Natural population analysis, J. Chem. Phys. (83) (2) (1985) 735-746. doi: 10.1063/1.449486.

[40] G. Schaftenaar, J.H. Noordik, Molden: a pre- and post-processing program for molecular and electronic structures, J. Comput.-Aided Mol. Design (14) (2) (2000) 123-134. doi: 10.1023/A:1008193805436.

HIGHLIGHTS

- Phyto-toxic activity of compounds **A-D** was evaluated.
- Docking was performed against possible target.
- Spectroscopic data are presented and discussed.
- DFT approach was applied for computational analysis.